ACS APPLIED MATERIALS & INTERFACES

Letter

www.acsami.org

Glucosamine-Anchored Graphene Oxide Nanosheets: Fabrication, Ultraviolet Irradiation, and Electrochemical Properties

Murugan Veerapandian,[†] Nicolas Lévaray,[†] Min-Ho Lee,[‡] Suzanne Giasson,*[,†,§] and X. X. Zhu*[,†]

[†]Department of Chemistry and [§]Faculty of Pharmacy, Université de Montréal, C.P. 6128, Succursale Centre-ville, Montreal, Quebec H3C 3J7, Canada

[‡]Medical IT Technology, Korea Electronics Technology Institute, Gyeonggi-do 463-816, Republic of Korea

Supporting Information

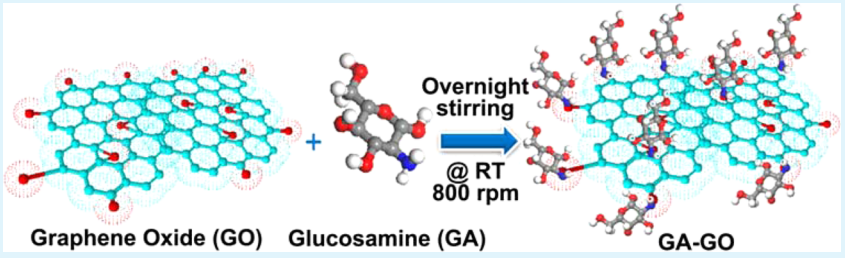

ABSTRACT: A biofunctionalized graphene oxide (GO) nanosheet with improved physicochemical properties is useful for electrocatalysis and sensor development. Herein, a new class of functionalized GO with a chemically anchored biomolecule glucosamine is developed. Structural and chemical analyses confirm the glucosamine anchoring. Ultraviolet irradiation transforms the surface chemistry of GO. Glucosamine-anchored GO nanosheets exhibit improved cyclic voltammetric and amperometric sensing activity toward the model redox probe, ruthenium(II) and *N*-acetylneuraminic acid, respectively. The biomolecular anchoring and ultraviolet irradiation helped to tune and enhance the properties of GO, which may find multiple applications in optimizing sensor platforms.

KEYWORDS: *graphene oxide, glucosamine, ultraviolet irradiation, photoluminescence, cyclic voltammetry, amperometric sensing*

Two-dimensional graphene oxide (GO) nanosheets garnered recent attention for multidisciplinary applications because of their cost-effective fabrication, ultrathin layers, large surface area, ease of surface modification, energy storage, and conversion.[1,2] GO is a chemical derivative of graphene possessing a variety of chemically reactive oxygen groups.[3] Depending on the nature and fraction of the sp^2/sp^3 carbon atomic ratio, the optical, bioaffinity, and electrochemical properties of GO could be effectively tuned for device development in optoelectronics, photoelectrochemical systems, and biosensors.[4−6] Elemental doping and chemical conjugation of organic molecules on GO are the general approaches to improve the physicochemical properties of GO.[7−10] In particular, doping of electron-accepting nitrogen atoms is regarded as an effective method to vary the physicochemical properties of GO.[8,9,11] The incorporation of nitrogen atoms imparts a relatively high positive charge density to adjacent carbon atoms and creates an altered bonding configuration within the carbon lattice and high electrocatalytic activity.[9,11] Nitrogen doping often utilizes chemical reagents such as ammonia, ammonia/methane mixture, acetonitrile, melamine, pyridine, hydrazine, and lithium nitride.[8] Compared with conventional chemical doping or treatment, photoirradiation is regarded as an ecofriendly and easy method to optimize the functional groups of GO suitable for device development.[12,13] For instance, ultraviolet (UV) photoirradiation induced a significant modification on the surface chemistry of GO sheets, mediated by the reduction of oxygen functional groups in the sp^3 regions of GO.[14] UV-irradiated GO showed a dramatic increase in the electrical conductivity similar to a semimetal, whereas pristine GO was nearly insulating.[15] From these studies, it is obvious that the fabrication of novel functionalized GO nanosheets and UV photoirradiation are potential strategies to explore multidisciplinary applications.

Glucosamine (GA) is an important amino sugar, and its functionalization on transition-metal nano/microstructures may enhance the surface wettability, crystallinity, and thermal, electrochemical, optical, and antibacterial properties of the final material.[15,16] UV irradiation on GA-modified copper nanoparticles has been shown to enhance photoluminescence (PL), electronic state, and reactive oxygen species suitable for antibacterial materials.[17] Here, GA is used for the first time as a "functional anchor" to create novel functionalized GO. The $-NH_2$ group of GA is expected to provide significant modification in the nonoxygenated and oxygenated regions of GO. UV irradiation is employed on the surface of the GA-functionalized GO (GA-GO), and the resulting changes in the optical and structural properties associated with bond

Received: January 29, 2015
Accepted: June 29, 2015
Published: June 29, 2015

DOI: 10.1021/acsami.5b00608
ACS Appl. Mater. Interfaces 2015, 7, 14552−14556

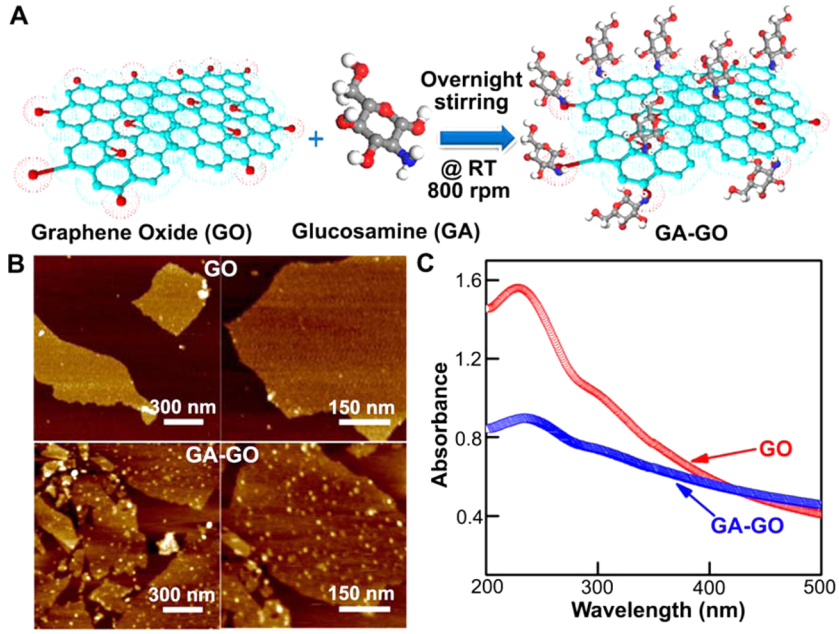

Figure 1. (A) Schematic illustration of GA anchoring on the surface of a GO nanosheet (cyan, carbon in GO; gray, carbon in GA; red, oxygen; white, hydrogen; blue, nitrogen). (B) AFM images. (C) UV−vis absorbance spectra.

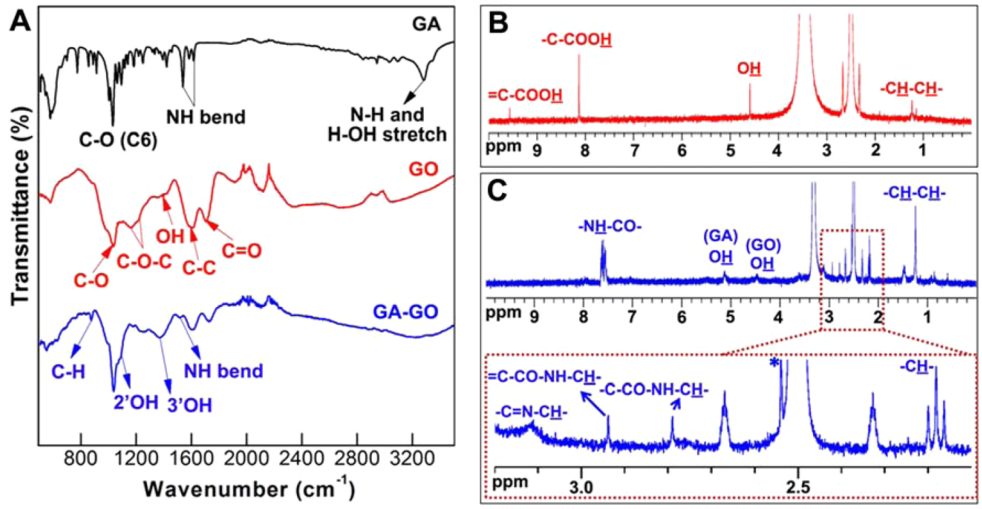

Figure 2. (A) Attenuated total reflectance FT-IR spectra. The GA spectrum with assigned functional groups is coherent with the reported literature.[16] ^{1}H NMR spectra of GO (B) and GA-GO nanosheets (C). The asterisk denotes the C-2 proton of GA associated with the epoxide ring-opening reaction.

distortions and restorations are compared with those of pristine GO. For proof-of-concept, the cyclic voltammetry and amperometric sensing abilities of UV-irradiated GA-GO were demonstrated using a model redox probe [ruthenium(II) complex] and *N*-acetylneuraminic acid (NANA). Because of its photosensitive and redox-active nature, catalytic oxidation of the ruthenium(II) complex is often used in biodetection,[18] photovoltaics, and organic light-emitting diodes.[19] NANA is a carbohydrate moiety found in mammalian cells and is recognized as the vital marker for tumor malignancy, diabetic symptoms, and cardiovascular disease, as reviewed elsewhere in the literature.[20] The UV-irradiated GA-GO electrode was modified by physicosorption through drop casting of an enzyme NANA aldolase to detect free NANA. Comparative analyses of the structural, optical, and electrochemical properties may help to gain insight into biofunctionalization of the GO nanosheets.

Figure 1A depicts the reaction and surface anchoring of GA on the basal planes and edges of a GO nanosheet. Chemically reactive oxygen groups at the edges and basal planes of GO may mediate multiple reactions with an amine group of GA such as amidation via covalent reaction with the carboxylic group of GO. Furthermore, the presence of epoxy groups on the basal planes of GO mediates the ring-opening reaction through nucleophilic attack at the α-carbon by the amine group[21] of GA. This favors the chemical anchoring of GA on GO sheets. The chemical structures of oxygenated functional groups of GO and its chemical bonding with the $-NH_2$ group of GA (before and after UV irradiation) are shown in Figure S4 in the Supporting Information (SI). The surface modification of GO sheets by GA is studied by atomic force microscopy

DOI: 10.1021/acsami.5b00608
ACS Appl. Mater. Interfaces 2015, 7, 14552−14556

(AFM) and UV−vis, FT-IR, Raman, and NMR spectroscopies. The AFM images show the sheetlike structures with sharp edges in the GO (Figure 1B, top). The successful anchoring of GA on the surface of GO nanosheets can be observed by the bright spots ascribed to the clusters of GA molecules (Figure 1B, bottom). Cross-sectional analysis further supported the morphological information by the change observed by AFM in the layer thickness (Figure S1 in the SI). The UV−vis spectra in Figure 1C show that the surface modification of GO with GA results in a slightly broadened absorption peak centered at 235 nm, corresponding to the $\pi \rightarrow \pi^*$ transition of the aromatic C−C bonds.[22]

The FT-IR spectra in Figure 2A show that GA anchoring on the surface of GO nanosheets yields noticeable structural changes to the final material such as the appearance of a new peak at 1521 cm^{-1} attributed to a secondary amine NH bend.[23] As expected, the reaction between the $-NH_2$ group of GA and the carboxylic group of GO results in a peak shift and broadening of C═O (carboxylic acid) bending vibrations located at 1730 cm^{-1}. The short peak at 874 cm^{-1} and the shoulder at 1090 cm^{-1} are ascribed to a C−H out-of-plane bend[23] and a secondary OH group of GA, respectively. Weakened epoxy group signals at 1180 and 1255 cm^{-1} and the formation of a broad peak centered at 1368 cm^{-1} associated with a tertiary OH group are signs of a probable ring-opening reaction between the epoxy group at the basal planes of GO and the $-NH_2$ group of GA.

The chemical reactivity of GO nanosheets strongly depends on the surface coverage of the oxygen groups.[3] Anchoring of GA on GO nanosheets modified the ^1H NMR shifts of characteristic functional groups in GO including COOH to CONH (Figure 2C). The reduction of the OH signal of GO and the appearance of new characteristic peaks at 3.1, 2.9, and 2.8 ppm also indicate the anchoring of GA molecules on the surface of GO.

Raman spectroscopy was used to elucidate the structural integrity between GO and GA-GO. It is known that Raman spectra of carbon materials exhibit a G band at ∼1580 cm^{-1} corresponding to the optical mode vibration of two neighboring carbon atoms and a D band at ∼1350 cm^{-1} corresponding to defects in graphene.[24] Changes in the position, shape, and intensity of these bands indicate functionalization and/or topological distortion on the graphitic layers. For instance, a shift of the G-band peak position from a lower wavenumber to a higher wavenumber indicates the oxidation of graphite, and the existence of a D band indicates the formation of local defects and disorder in the graphitic layers.[14]

In Figure 3, pristine GO exhibits a G band at 1596 cm^{-1} that is blue-shifted from the inherent G peak (∼1580 cm^{-1})[21] of the carbon lattice, revealing the oxygenation of graphite and formation of sp^3 carbon atoms. The D band in pristine GO at 1356 cm^{-1} indicates the reduction of in-plane sp^2 regions mediated by the formation of distortions, vacancies, and defects during oxidation. In the case of UV-irradiated GO, the G band is shifted toward a lower wavenumber (1592 cm^{-1}) because of the regraphitization that results in the formation of more sp^2 carbon atoms. The ratio of the intensities of the D and G bands (I_D/I_G) are shown in Figure 3 (bottom). The I_D/I_G ratio is inversely proportional to the in-plane sp^2 graphitic domains.[24] Herein, a decrease in the intensity ratio I_D/I_G from 0.81 to 0.75 indicates that UV irradiation has altered the surface chemistry of GO by forming large sp^2 domains, which agrees well with the X-ray photoelectron spectroscopy (XPS) results (Figures S3 and S5 in the SI). A similar trend was reported by Matsumoto et al., where the I_D/I_G ratio decreases from 1.12 to 1.02 and 1.03 after 2 h of photoreduction of GO in H_2 and N_2, respectively.[14] It is worth mentioning that, in addition to the functional groups of the sample, the duration of UV irradiation, wavelength/intensity of the source, and distance between the source and sample are important parameters influencing the structural variations and I_D/I_G ratio. In this study, an UV irradiation lamp with a short wavelength of ∼254 nm and a preset energy of 10 $\mu J/cm^2$ is used for 30 min in ambient conditions. GA anchoring on GO shifted the G-band position to 1599 cm^{-1} and increased the peak intensity of the D band at 1358 cm^{-1}. The I_D/I_G ratios of GA-GO and UV-irradiated GA-GO were found to be 0.83 and 0.79, respectively. These results suggest that GA anchoring has promoted the formation of new sp^3 domains on the GO lattice via C−N bonding. Further, the UV irradiation process resulted in alteration of the residual oxygen groups and thereby mediated large sp^2 domains through photoreduction. Such modified sp^2/sp^3 domains on the GO lattice structures possess chemical compositions useful for enhancing the optical and electrochemical properties discussed in the following sections.

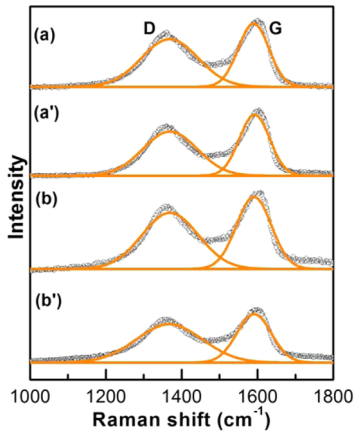

Sample	D	G	I_D/I_G ratio
(a)	1356	1596	0.81
(a')	1353	1592	0.75
(b)	1358	1599	0.83
(b')	1354	1593	0.79

Figure 3. Top: Raman spectra of GO [(a) before and (a′) after UV] and GA-GO [(b) before and (b′) after UV] nanosheets. The experimental data curve and Gaussian fitting curves are shown in black and orange, respectively. Bottom: Peak positions of the D and G bands and I_D/I_G ratios obtained after a Gaussian fit.

Chemical treatment and photoirradiation on GO modified the oxygen-containing functional groups, which resulted in modulation of the PL property.[4,25] Figure 4A shows the broad visible PL peak from GO centered at ∼725 nm, using an excitation wavelength of 514 nm, in agreement with an earlier study.[26] GA anchoring on the surface of GO resulted in a red shift of ∼25 nm, related to the new sp^3 domains on the graphite lattice formed by the functional groups of GA. Upon UV irradiation, both GO and GA-GO nanosheets show significant decreases in their emission peak intensity. However, GO exhibits a red shift at 730 nm, whereas GA-GO exhibits a blue shift at 740 nm. The quenching of the PL from UV-irradiated GO and GA-GO nanosheets might be related to the removal of oxygen functional groups and the restoration of additional sp^2

DOI: 10.1021/acsami.5b00608
ACS Appl. Mater. Interfaces 2015, 7, 14552−14556

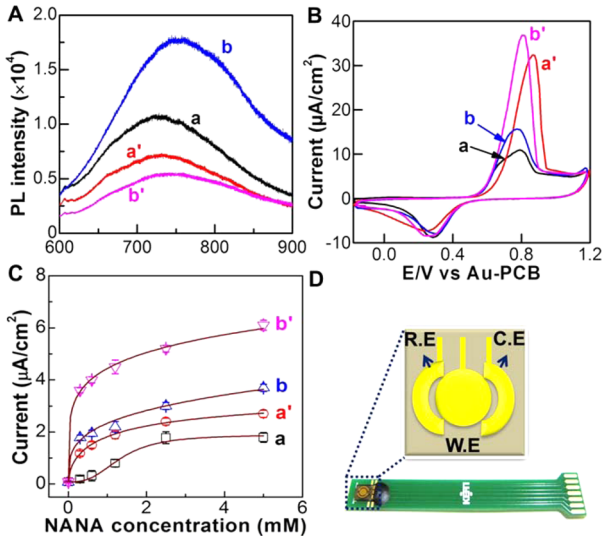

Figure 4. (A) PL spectra of GO-based materials: (a) pristine GO; (a′) UV-irradiated GO; (b) GA-GO; (b′) UV-irradiated GA-GO. (B) Cyclic voltammetry of different electrodes in 5 mM $[Ru(bpy)_3]^{2+}$ containing a 10 mM phosphate-buffered saline (PBS) solution (pH 7.4), at a scan rate of 50 mV/s. (C) Calibration curve fit illustrating the amperometric current of different electrodes modified with NANA aldolase against various concentrations of free NANA in PBS (10 mM, pH 7.4), at an applied bias of +0.7 V. Each data point represents the average of three independent measurements at different electrodes, and error bars represent the standard deviation of the mean. The current sensitivities measured as the slope of the plot were 1.82, 2.52, 3.23, and 5.24 μA/mM for GO, UV-irradiated GO, GA-GO, and UV-irradiated GA-GO modified electrodes, respectively. (D) Digital photo of the Au-PCB chip and an illustration depicting the electrode configuration (RE = reference electrode, CE = counter electrode, and WE = working electrode).

clusters in the GO sheets. Because of the distinct chemical composition of GA-GO, UV irradiation activated a larger amount of sp^2 clusters than sp^3 clusters on the surface of pristine GA-GO. The variation in the sp^2/sp^3 configuration caused a change in the carrier confinement of UV-irradiated GA-GO, resulting in a noticeable quenching of the PL compared to UV-treated GO. This is supported by the results of FT-IR (Figure 2A), ^1H NMR (Figure 2B), Raman (Figure 3), and XPS (Figures S3, S5, and S6 in the SI) studies.

To demonstrate the functional properties derived from GA anchoring and UV irradiation on a GO lattice, a prototype electrode was constructed using a customized gold-printed circuit board (Au-PCB) chip. Au-PCB electrodes modified with pristine GO, UV-irradiated GO, GA-GO, and UV-irradiated GA-GO were used for electrochemical measurements. Figure 4B shows the cyclic voltammograms obtained for 5 mM $[Ru(bpy)_3]^{2+}$ in 10 mM PBS (pH 7.4) with the four different electrodes. The pristine GO electrode showed an oxidation peak current of 10.7 μA/cm² for $[Ru(bpy)_3]^{2+}$. Anchoring of GA on GO nanosheets increased the oxidation peak current to 15.7 μA/cm² (curve b). This enhanced electronic property of GA-GO is most probably associated with the configuration of the C−N bond on the lattice, which provides the new sp^3 and sp^2 domains, lattice orientation, and its derived electroactive charge carriers. Because nitrogen has a larger electronegativity than carbon, electrons transfer from the carbon atoms to the nitrogen atoms and nitrogen back-donates electrons to adjacent C p_z orbitals. The electron donation and back-donation process facilitates O_2 dissociation on the neighboring carbon atoms.[27] Therefore, nitrogen species located at the edges and basal planes of the GO layers can easily contribute to the electron transfer through the carbon surface with high current density.[28] For instance, nitrogen-doped graphene from solvothermal synthesis[27] and plasma treatement[29] was found to facilitate the oxygen reduction reaction. Nitrogen doping also increases the atomic charge density and introduces asymmetry into the spin density on the graphene network,[30] which may help charge transfer from the carbon support to the adsorbing molecules and lead to an enhanced electrooxidation of $[Ru(bpy)_3]^{2+}$. The UV-irradiated GA-GO electrode shows an increased peak current associated with lower oxidation peak potential (b′: 800 mV), indicating a better electron-transfer process than that of the UV-irradiated GO electrode (a′: 870 mV) toward the oxidation of $[Ru(bpy)_3]^{2+}$. This enhanced redox behavior may be due to the incorporation of nitrogen atoms of GA molecules on the graphitic plane. The UV-irradiated GO and GA-GO electrodes significantly increased the peak current densities for the oxidation of $[Ru(bpy)_3]^{2+}$ such as 32.4 and 36.9 μA/cm², respectively. As discussed previously, UV irradiation induced the restoration of sp^2 clusters through the removal of residual oxygen groups on the basal planes and edges,[14] which, in turn, activated the charge carriers for rapid electron transfer. Figure S4 in the SI shows the chemical structure of UV-irradiated GA-GO, denoting the chemical bonding between the $-NH_2$ group of GA and the oxygenated functional groups of GO. Enhanced voltammetric behavior of GA-anchored GO is expected to have potential applications in the development of metal-free electrocatalysts, molecular sensing, and fuel cells.

Herein, the electrochemical sensing ability of the UV-irradiated GA-GO electrode was evaluated using an enzyme NANA aldolase, which catalyzes the following reversible reaction.

N-acetylneuraminic acid

↔ *N*-acetylmannosamine + pyruvate

The presence of NANA aldolase enzyme on the electrode surface readily oxidizes free NANA and hence supplies electrons to the electrode. Figure 4C shows the calibration curves obtained from the amperometric response of the electrodes to different concentrations of NANA. The UV-irradiated GA-GO/NANA aldolase electrode exhibits a significant enhancement in the amperometric current with different concentrations of NANA, which is superior to the other electrodes. This could be ascribed to the distinct surface chemistry obtained from the anchoring of GA on GO nanosheets.

In summary, a new biofunctionalization strategy using a biological amino sugar GA to enhance the voltammetric and amperometric sensing ability of GO nanosheets was developed. Chemically anchored GA formed new sp^3 domains on the GO lattice, which is beneficial for enhancing the PL properties. UV irradiation on GO and GA-GO alters the surface chemistry and offers new approaches for optimizing the electronic state. The UV-irradiated GA-GO electrode exhibited an increased oxidation current for $[Ru(bpy)_3]^{2+}$ and characteristic amperometric response to free NANA in a concentration dependence, which is superior to that of pristine GO, UV-irradiated GO, and pristine GA-GO electrodes. Studies on the effect of UV irradiation on other nitrogen-containing biomolecules on GO are in progress.

DOI: 10.1021/acsami.5b00608
ACS Appl. Mater. Interfaces 2015, 7, 14552−14556

■ ASSOCIATED CONTENT

Supporting Information

Experimental procedure for the synthesis of GA-GO nanosheets, information on UV irradiation, electrode fabrication, instrumental characterization, ζ potential, AFM cross-sectional analysis, XPS, cyclic voltammograms, electroactive area, and electron-transfer rate constants. The Supporting Information is available free of charge on the ACS Publications website at DOI: 10.1021/acsami.5b00608.

■ AUTHOR INFORMATION

Corresponding Authors

*E-mail: suzanne.giasson@umontreal.ca.

*E-mail: julian.zhu@umontreal.ca.

Notes

The authors declare no competing financial interest.

■ ACKNOWLEDGMENTS

Financial support from NSERC of Canada and FRSQ and FQRNT of Quebec is acknowledged. M.V. thanks the GRSTB for a postdoctoral scholarship. The authors are members of GRSTB funded by FRSQ.

■ REFERENCES

(1) Kumar, P. V.; Bardhan, N. M.; Tongay, S.; Wu, J.; Belcher, A.; Grossman, J. C. Scalable Enhancement of Graphene Oxide Properties by Thermally Driven Phase. *Nat. Chem.* **2014**, *6*, 151−158.

(2) Eda, G.; Lin, Y. Y.; Mattevi, C.; Yamaguchi, H.; Chen, H. A.; Chen, I. S.; Chen, C. W.; Chhowalla, M. Blue Photoluminescence from Chemically Derived Graphene Oxide. *Adv. Mater.* **2010**, *22*, 505−509.

(3) Dreyer, D. R.; Park, S.; Bielawski, C. W.; Ruoff, R. S. The Chemistry of Graphene Oxide. *Chem. Soc. Rev.* **2010**, *39*, 228−240.

(4) Li, M.; Cushing, S. K.; Zhou, X.; Guo, S.; Wu, N. Fingerprinting Photoluminescence of Functional Groups in Graphene Oxide. *J. Mater. Chem.* **2012**, *22*, 23374−23379.

(5) Veerapandian, M.; Seo, Y.-T.; Yun, K. S.; Lee, M.-H. Graphene Oxide Functionalized with Silver@Silica−Polyethylene Glycol Hybrid Nanoparticles for Direct Electrochemical Detection of Quercetin. *Biosens. Bioelectron.* **2014**, *58*, 200−204.

(6) Devadoss, A.; Sudhagar, P.; Das, S.; Lee, S. Y.; Terashima, C.; Nakata, K.; Fujishima, A.; Choi, W.; Kang, Y. S.; Paik, U. Synergistic Metal−Metal Oxide Nanoparticles Supported Electrocatalytic Graphene for Improved Photoelectrochemical Glucose Oxidation. *ACS Appl. Mater. Interfaces* **2014**, *6*, 4864−4871.

(7) Georgakilas, V.; Otyepka, M.; Bourlinos, A. B.; Chandra, V.; Kim, N.; Kemp, K. C.; Hobza, P.; Zboril, R.; Kim, K. S. Functionalization of Graphene: Covalent and Non-Covalent Approaches, Derivatives and Applications. *Chem. Rev.* **2012**, *112*, 6156−6214.

(8) Wang, H.; Maiyalagan, T.; Wang, X. Review on Recent Progress in Nitrogen-Doped Graphene: Synthesis, Characterization, and Its Potential Applications. *ACS Catal.* **2012**, *2*, 781−794.

(9) Van Khai, T.; Na, H. G.; Kwak, D. S.; Kwon, Y. J.; Ham, H.; Shim, K. B.; Kim, H. W. Influence of N-Doping on the Structural and Photoluminescence Properties of Graphene Oxide Films. *Carbon* **2012**, *50*, 3799−3806.

(10) Krishnamoorthy, K.; Jeyasubramanian, K.; Premanathan, M.; Subbiah, G.; Shin, H. S.; Kim, S. J. Graphene Oxide Nanopaint. *Carbon* **2014**, *72*, 328−337.

(11) He, D.; Jiang, Y.; Lv, H.; Pan, M.; Mu, S. Nitrogen-Doped Reduced Graphene Oxide Supports for Noble Metal Catalysts with Greatly Enhanced Activity and Stability. *Appl. Catal., B* **2013**, *132*, 379−388.

(12) Cote, L. J.; Cruz−Silva, R.; Huang, J. X. Flash Reduction and Patterning of Graphite Oxide and Its Polymer Composite. *J. Am. Chem. Soc.* **2009**, *131*, 11027−11032.

(13) Sun, H.; Wu, Li.; Gao, N.; Ren, J.; Qu, X. Improvement of Photoluminescence of Graphene Quantum Dots with A Biocompatible Photochemical Reduction Pathway and Its Bioimaging Application. *ACS Appl. Mater. Interfaces* **2013**, *5*, 1174−1179.

(14) Matsumoto, Y.; Koinuma, M.; Kim, S. Y.; Watanabe, Y.; Taniguchi, T.; Hatakeyama, K.; Tateishi, H.; Ida, S. Simple Photoreduction of Graphene Oxide Nanosheet Under Mild Conditions. *ACS Appl. Mater. Interfaces* **2010**, *2*, 3461−3466.

(15) Veerapandian, M.; Lim, S. K.; Nam, H. M.; Kuppannan, G.; Yun, K. S. Glucosamine Functionalized Silver Glyconanoparticles: Characterization and Antibacterial Activity. *Anal. Bioanal. Chem.* **2010**, *398*, 867−876.

(16) Veerapandian, M.; Subbiah, R.; Lim, G. S.; Park, S. H.; Yun, K. S.; Lee, M. H. Copper-Glucosamine Microcubes: Synthesis, Characterization, and C-Reactive Protein Detection. *Langmuir* **2011**, *27*, 8934−8942.

(17) Veerapandian, M.; Sadhasivam, S.; Choi, J. H.; Yun, K. S. Glucosamine Functionalized Copper Nanoparticles: Preparation, Characterization and Enhancement of Anti-Bacterial Activity by Ultraviolet Irradiation. *Chem. Eng. J.* **2012**, *209*, 558−567.

(18) Veerapandian, M.; Zhu, X. X.; Giasson, S. Chitosan-modified Silver@Ruthenium Hybrid Nanoparticles: Evaluation of Physico-Chemical Properties and Bio-Affinity with Sialic Acid. *J. Mater. Chem. B* **2015**, *3*, 665−672.

(19) Kalyanasundaram, K. Photophysics, Photochemistry and Solar Energy Conversion with Tris(bipyridyl)ruthenium(II) and Its Analogues. *Coord. Chem. Rev.* **1982**, *46*, 159−244.

(20) Marzouk, S. A. M.; Ashraf, S. S.; Al Tayyari, K. A. Prototype Amperometric Biosensor for Sialic Acid Determination. *Anal. Chem.* **2007**, *79*, 1668−1674.

(21) Wang, S.; Chia, P. J.; Chua, L. L.; Zhao, L. H.; Png, R.-Q.; Sivaramakrishnan, S.; Zhou, M.; Goh, R.G.-S.; Friend, R. H.; Wee, A.T.-S.; Ho, P.K.-H. Band-like Transport in Surface Functionalized Highly Solution-Processable Graphene Nanosheets. *Adv. Mater.* **2008**, *20*, 3440−3446.

(22) Zhang, D.; Liu, X.; Wang, X. Green Synthesis of Graphene Oxide Sheets Decorated by Silver Nanoprisms and Their Anti-Bacterial Properties. *J. Inorg. Biochem.* **2011**, *105*, 1181−1186.

(23) Coates, J. In *Encyclopedia of Analytical Chemistry*; Meyers, R. A., Ed.; John Wiley & Sons: Chichester, U.K., 2000; pp 10815−10837.

(24) Ferrari, A. C.; Robertson, J. Interpretation of Raman Spectra of Disordered and Amorphous Carbon. *Phys. Rev. B: Condens. Matter Mater. Phys.* **2000**, *61*, 14095−14107.

(25) Kumar, P.; Subrahmanyam, K. S.; Rao, C. N. R. Graphene Produced by Radiation-Induced Reduction of Graphene Oxide. *Int. J. Nanosci.* **2011**, *10*, 559−566.

(26) Luo, Z.; Vora, P. M.; Mele, E. J.; Johnson, A. T. C.; Kikkawa, J. M. Photoluminescence and Band Gap Modulation in Graphene Oxide. *Appl. Phys. Lett.* **2009**, *94*, 111909.

(27) Deng, D.; Pan, X.; Yu, L.; Cui, Y.; Jiang, Y.; Qi, J.; Li, W.-X.; Fu, Q.; Ma, X.; Xue, Q.; Sun, G.; Bao, X. Toward N-doped Graphene via Solvothermal Synthesis. *Chem. Mater.* **2011**, *23*, 1188−1193.

(28) Lee, K. H.; Oh, J.; Son, J. G.; Kim, H.; Lee, S.-S. Nitrogen-doped Graphene Nanosheets from Bulk Graphite Using Microwave Irradiation. *ACS Appl. Mater. Interfaces* **2014**, *6*, 6361−6368.

(29) Imran Jafri, R.; Rajalakshmi, N.; Ramaprabhu, S. Nitrogen Doped Graphene Nanoplatelets as Catalyst Support for Oxygen Reduction Reaction in Proton Exchange Membrane Fuel Cell. *J. Mater. Chem.* **2010**, *20*, 7114−7117.

(30) Kannan, P.; Maiyalagan, T.; Sahoo, N. G.; Opallo, M. Nitrogen Doped Graphene Nanosheet Supported Platinum Nanoparticles as High Performance Electrochemical Homocysteine Biosensors. *J. Mater. Chem. B* **2013**, *1*, 4655−4666.

DOI: 10.1021/acsami.5b00608
ACS Appl. Mater. Interfaces 2015, 7, 14552−14556